nature ecology & evolution

SUPPLEMENTARY INFORMATION

https://doi.org/10.1038/s41559-018-0722-0

In the format provided by the authors and unedited.

Evolution and extinction of the giant rhinoceros *Elasmotherium sibiricum* sheds light on late Quaternary megafaunal extinctions

Pavel Kosintsev[1], Kieren J. Mitchell[2], Thibaut Devièse[3], Johannes van der Plicht[4,5], Margot Kuitems[4,5], Ekaterina Petrova[6], Alexei Tikhonov[6], Thomas Higham[3], Daniel Comeskey[3], Chris Turney[7,8], Alan Cooper[2], Thijs van Kolfschoten[5], Anthony J. Stuart[9] and Adrian M. Lister[10]*

[1]Institute of Plant and Animal Ecology, Ural Branch of the Russian Academy of Sciences, Yekaterinburg, Russia. [2]Australian Centre for Ancient DNA, School of Biological Sciences, University of Adelaide, Adelaide, Australia. [3]Oxford Radiocarbon Accelerator Unit, University of Oxford, Oxford, UK. [4]Center for Isotope Research, Groningen University, Groningen, The Netherlands. [5]Faculty of Archaeology, Leiden University, Leiden, The Netherlands. [6]Zoological Institute, Russian Academy of Sciences, Saint Petersburg, Russia. [7]Palaeontology, Geobiology and Earth Archives Research Centre, School of Biological, Earth and Environmental Sciences, University of New South Wales, Sydney, Australia. [8]Climate Change Research Centre, School of Biological, Earth and Environmental Sciences, University of New South Wales, Sydney, Australia. [9]Department of Biosciences, Durham University, Durham, UK. [10]Department of Earth Sciences, Natural History Museum, London, UK. *e-mail: A.Lister@nhm.ac.uk

Evolution and extinction of the giant rhinoceros *Elasmotherium sibiricum* sheds light on late Quaternary megafaunal extinctions

Supplementary Information

Pavel Kosintsev[1], Kieren J. Mitchell[2], Thibaut Devièse[3], Johannes van der Plicht[4,5], Margot Kuitems[4,5], Ekaterina Petrova[6], Alexei Tikhonov[6], Thomas Higham[3], Daniel Comeskey[3], Chris Turney[7], Alan Cooper[2], Thijs van Kolfschoten[5], Anthony J Stuart[8], Adrian M Lister[9*].

[1] Institute of Plant and Animal Ecology, Ural Branch, Russian Academy of Sciences, 8 Marta St. 202, Yekaterinburg 620144, Russia

[2] Australian Centre for Ancient DNA, School of Biological Sciences, University of Adelaide, North Terrace Campus, South Australia 5005, Australia

[3]Oxford Radiocarbon Accelerator Unit, University of Oxford, 1-2 South Parks Road, Oxford, OX1 3TG, UK

[4] Center for Isotope Research, Groningen University, Groningen, The Netherlands

[5] Faculty of Archaeology, Leiden University, P.O. Box 9514, 2300 RA Leiden, The Netherlands

[6] Zoological Institute, Russian Academy of Sciences, 1 Universitetskaya Naberezhnaya, St. Petersburg, 199034, Russia

[7] Palaeontology, Geobiology and Earth Archives Research Centre, and Climate Change Research Centre, School of Biological, Earth, and Environmental Sciences, University of New South Wales, Sydney, Australia.

[8] Department of Biosciences, Durham University, South Road, Durham DH1 3LE, UK

[9] Department of Earth Sciences, Natural History Museum, London SW7 5BD, UK

1. **Sample provenances and palaeoenvironments** (by Pavel Kosintsev)

The samples utilized in the present study came from the following locations:

Tobolsk (58° N 68° E). A total of 368 mammalian remains were recovered from this locality. *Elasmotherium* is represented by a radius - the northernmost finding of the *E. sibiricum*. Other species include *Mammuthus primigenius*, *Equus ferus*, *Coelodonta antiquitatis*, *Rangifer tarandus*, *Bison priscus* and *Saiga tatarica* (Kosintsev & Bobkovskaya, 2003).

Irbit (57° 40' 63° 04'). Five bones were found, belonging to *Mammuthus primigenius*, *Coelodonta antiquitatis* and *Elasmotherium sibiricum*. *Elasmotherium* is represented by a skull fragment.

Borovlyanka (56° 48'N 62° 52'E). The remains, consisting of 92 bones, belong to *Mammuthus primigenius*, *Equus ferus*, *Coelodonta antiquitatis*, *Elasmotherium sibiricum*, *Rangifer tarandus* and *Bison priscus*. *Elasmotherium* is represented by a first lower molar and metacarpal IV.

Voronovka (55° 27'N 65° 20'E). The collection consists of 357 bones. Mammalian remains include *Mammuthus primigenius*, *Equus ferus*, *Coelodonta antiquitatis*, *Elasmotherium sibiricum*, *Rangifer tarandus*, *Bison priscus* and *Saiga tatarica*. *Elasmotherium* is represented by a skull fragment. A radiocarbon date obtained on a mammoth bone is 41,000±650 (SOAN-5643), on a rhinoceros bone, 17,200±150 (SOAN-5644), and on a bison bone, 12,505±55 (OxA-14948).

Smelovskaya II cave (53°36' N, 58°54' E). Cave deposits consist of five layers. Radiocarbon dates from layer 1 correspond to the Holocene, while layers 2 – 4 are dated to the Late Pleistocene. From layer 5 no animal remains were obtained. Samples of mammal bones from layers 2 – 3 yielded radiocarbon dates of 15,590±150 (LE-2774); 25,000±600 (GIN-8403); 31,000±1500 (GIN-8401) and 41,000±1800 (GIN-8402) (Sinitsyn & Praslov, 1997).

In layer 4, a single tooth of *Elasmotherium* was found in association with steppe pika (*Ochotona pusilla*), hare (*Lepus timidus*), bobak marmot (*Marmota bobak*), wolf (*Canis lupus*), arctic fox (*Vulpes lagopus*), red fox (*Vulpes vulpes*), corsac fox (*Vulpes corsac*), cave lion (*Panthera spelaea*), cave hyena (*Crocuta crocuta spelaea*), mammoth (*Mammuthus primigenius*), wild horse (*Equus ferus*), wooly rhinoceros (*Coelodonta antquitatis*), red deer (*Cervus elaphus*), giant deer (*Megaloceros giganteus*), steppe bison (*Bison priscus*) and saiga (*Saiga tatarica*). From layer 4 were obtained radiocarbon dates of >59,800 (OxA-19535) and >60,800 (OxA-19534) on bones of cave hyena, and >47,800 (OxA-27616) on giant deer.

Belaya river, Bashkiriya (several localities 53-55° N 55-57° E). In all 14 bones were found in alluvial deposits of the Belaya River, belonging to *Mammuthus primigenius*, *Equus ferus*, *Coelodonta antiquitatis*, *Elasmotherium sibiricum* and *Bison priscus*. *Elasmotherium* is represented by fragments of two skulls and three teeth (M2, m1, m2).

Saratov (51° 31' N, 46° 00' E). There are several localities with fossil remains near Saratov on the banks of the Volga river, where bones of *Mammuthus trogontherii*, *Mammuthus primigenius*, *Equus ferus*, *Coelodonta antiquitatis*, *Elasmotherium sibiricum*, *Camelus knoblochi*, *Megaloceros giganteus*, *Cervus elaphus* and *Bison priscus* have been collected (Khromov, 1999; Khromov et al. 2001). *Elasmotherium* is represented by a tooth.

Sarepta (48° 31' N, 44° 30' E). Fossil remains of *Panthera spelaea*, *Mammuthus* sp., *Equus ferus*, *Stephanorhinus* cf. *kirchbergensis*, *Elasmotherium sibiricum*, *Camelus knoblochi*, *Megaloceros giganteus*,

Cervus elaphus and *Bison priscus* were found on the banks of the Volga river at this locality (Gromova, 1932). *Elasmotherium* is represented by a largely complete cranium.

Luchka (Svetliy Yar) (48°28'N, 44°46'E). The specimen was found on the banks of the Volga River near the village of SvetliyYar (Volgograd Region). No further information is available.

Samara District (53°12'N, 50°6'E). The specimens were found on the banks of the Volga River near the city of Samara. No further information is available.

Odessa district (48°30N, 30°42E). The specimen was found near the city of Odessa. No further information is available.

Paleoenvironmental conditions for MIS 3 in the region of *Elasmotherium* distribution are based on palynological spectra, plant macrofossils, insect and mammal assemblages from many localities (Borodin et al., 2013; Danukalova et al., 2009; Grichuk, 2002; Ivakina et al., 1999. Khromov et al., 2000; Kosintsev, & Bachura, 2013; Kosintsev & Bobkovskaya, 2003; Kosintsev & Vasiliev, 2009; Markova et al., 2008; Markova et al., 2002; Shilova et al. 2008; Shirokov et al., 2011; Stefanovsky et al., 2002; 2003; 2007; Zinoviev, 2003; 2011).

The available data suggest the presence of semi-open landscapes in the Middle Volga and Ural region during MIS3. The closest modern analogy of this landscape is the forest steppe zone. The area was dominated by grasslands with Poaceae, Chenopodiaceae and mixed herbs. Tree vegetation included pine (*Pinus silvestris*), birch (*Betula* sec. *Albae*) and small numbers of deciduous species (*Quercus, Ulmus, Tilia*). The large mammal fauna was dominated by grazing species *Equus ferus*, *Coelodonta antiquitatis* and *Bison priscus* - the percentage of their bones in assemblages ranges from 70% to 90%. The proportion of *Mammuthus primigenius*, *Cervus elaphus*, *Megaloceros giganteus* and *Saiga tatarica* remains varies from 10% to 30%. In the small mammal assemblages *Ochotona pusilla, Lagurus lagurus, Eolagurus luteus* and *Microtus gregalis* represent about 80% of all remains, while *Spermophilus* sp., *Allactaga* sp., *Allactagulus* sp. and *Ellobius talpinus* comprise about 20% of all remains.

Open landscapes similar to modern steppes were present in the southern Trans-Urals during MIS3. The vegetation was dominated by Chenopodiaceae*, Artemisia sp.,* mixed herbs and grasses. Forests occurred on river floodplains and consisted of birch (*Betula* sec. *Albae*) and broad-leaved species (*Quercus, Ulmus, Tilia*). *Equus ferus*, *Coelodonta antiquitatis* and *Bison priscus* prevailed in faunal assemblages with approximately 90% of all large mammal remains. The percentage of other species – *Mammuthus primigenius, Cervus elaphus, Megaloceros giganteus, Saiga tatarica* – is about 10%. Small mammal assemblages contain a high percentage (about 90%) of *Lagurus lagurus, Eolagurus luteus*, and *Microtus gregalis* remains. The remains of *Ochotona pusilla*, *Spermophilus* sp., *Allactaga* sp., *Allactagulus* sp. and *Ellobius talpinus* comprise approximately 10%.

In the northern Trans-Urals and Western Siberia this period was characterized by forest-steppe landscapes, though forested areas were reduced during stadial periods. Plant communities with Chenopodiaceae and *Artemisia sp*. were present on the flat interfluves, while spruce, pine and birch forests grew in the lowlands and along rivers. In the interstadials they were replaced by pine and pine-birch mixed forest. The increasing moisture led to expansion of light-coniferous forest with fir and birch in the area. The majority of bones (about 90%) from these sites belong to *Mammuthus primigenius*, *Equus ferus*, *Coelodonta antiquitatis* and *Bison priscus*. Less common species like *Alces alces*, *Cervus elaphus*, *Megaloceros giganteus*, *Rangifer tarandus*, *Saiga tatarica* comprise a small part of large

mammal faunal assemblages (about 10%). Bone remains of *Lagurus lagurus* and *Microtus gregalis* make up almost 50% of all small mammal assemblages. Remains of *Ochotona pusilla*, *Spermophilus* sp., *Cricetulus migratorius*, *Clethrionomys* sp. and *Dicrostonyx gulielmi* comprise the other half (about 50%) of the samples.

The mammalian fauna from all regions also includes many additional Late Pleistocene species like *Canis lupus*, *Vulpes lagopus*, *Panhtera spelaea*, *Crocuta crocuta spelaea*, *Lepus timidus, Marmota bobak*, *Microtus oeconomus*, *Arvicola terrestris*.

In sum, pollen, floral and faunal data suggest that in the studied area *Elasmotherium sibiricum* inhabited the forest-steppe landscapes with extensive grasslands as well as wooded areas. Only in the southern Trans-Urals did it live in fully open steppe habitats.

Radiocarbon dates are tabulated in Supplementary Table 1.

2. **DNA Analysis** (by Kieren J. Mitchell and Alan Cooper)

DNA extraction

All ancient DNA (aDNA) extraction and library preparation steps reported in this paper were performed in a purpose-built, physically isolated, ancient DNA laboratory at the Australian Centre for Ancient DNA (ACAD), University of Adelaide. We reduced potential surface contamination of the *Elasmotherium sibiricum* bone samples by removing surfaces (~1 mm) using a Dremel tool and cutting wheel, followed by UV irradiation for 15 min. Each bone sample was then powdered using a mikrodismembrator (Sartorius), and 0.2 g was lysed by rotational incubation at 37 °C overnight in 4 mL of 0.5M EDTA pH 8.0, followed by a further incubation at 55 °C for 2 hr with the addition of 60 μL of proteinase-K. The released DNA was bound, washed, and eluted using a silica-based method (Brotherton et al., 2013).

In addition to the samples reported in this paper, a further two samples were assessed for DNA preservation (S. Brace, pers. comm.). DNA extraction (Dabney et al 2013) and library preparation steps (Meyer and Kircher 2010) were carried out on two samples, a molar (NHMUK PV M7099) from Saratov, and a cranium (NHMUK PV M12429) from Sarepta (see Supplementary Table 1) in the dedicated ancient DNA laboratory at the Natural History Museum, London. Unfortunately these samples contained insufficient yields of endogenous DNA for the samples to be taken forward for further analyses.

Library preparation and sequencing

Extracted DNA was enzymatically repaired and blunt-ended, and custom adapters ligated following the protocol of Meyer and Kircher (2010). Adapter sequences featured unique barcodes (single P5 5-mer barcodes for IPAE915/2804, IPAE897/123, IPAE2388/1, and IPAE2388/5; dual P5 and P7 7-mer barcodes for IPAE1871/200 and IPAE897/200) in order to allow identification and exclusion of any downstream contamination. Libraries were subjected to a short round of PCR in order to increase the total quantity of DNA using primers complementary to the adapter sequences. Cycle number was kept low and template was split into eight separate PCRs per library in order to minimise PCR bias and maintain library complexity. Each individual PCR (25 μL) contained 1× PCR buffer, 2.5 mM MgCl2, 1 mM dNTPs, 0.5 mM each primer, 0.1 U AmpliTaq Gold and 2 μL DNA library. Cycling conditions were as follows: 94

°C for 12 min; 12-13 cycles of 94 °C for 30 s, 60 °C for 30 s, 72 °C for 40 s (plus 2 s/cycle); and 72 °C for 10 min. PCR products were purified using AMPure magnetic beads (Agencourt).

Commercially synthesised biotinylated 80-mer RNA baits (MYcroarray, MI, USA) were used to enrich the target libraries for mitochondrial DNA. Baits were designed using published mitochondrial sequences from a range of placental mammals (see Mitchell et al., 2016a; Mitchell et al., 2016b). DNA-RNA hybridisation enrichment was performed according to manufacturer's recommendations (MYbaits protocol v1 for libraries IPAE915/2804, IPAE897/123, IPAE2388/1, and IPAE2388/5; MYbaits protocol v3 for libraries IPAE1871/200 and IPAE897/200) with the exception of the incubation step, which we extended to 44 hr (3 hr at 60°C, 12 hr at 55 °C, 12 hr at 50 °C, 17 hr at 55 °C). The quantity of DNA remaining after enrichment was extremely small, so an additional round of PCR was performed (12 cycles; conditions as above). Subsequently, a final round of PCR (7 cycles; conditions as above) was performed with fusion primers to add full-length Illumina sequencing adapters to the enriched libraries. The enriched libraries were diluted to 2 nM and run on an Illumina MiSeq using 2 x 150 bp (paired-end) sequencing chemistry.

Bioinformatic processing

Following sequencing, reads were demultiplexed according to the adapter barcode using 'sabre' (https://github.com/najoshi/sabre) (default parameters: no mismatches allowed). Adapter sequences were removed and paired-end reads were merged using Adapter Removal v2.1.2 (Lindgreen, 2012). Low quality bases were trimmed (<Phred20 --minquality 4) and merged reads shorter than 25 bp were discarded (--minlength 25). Read quality was visualized using fastQC v0.10.1 (http://www.bioinformatics.bbsrc.ac.uk/projects/fastqc) before and after trimming to make sure the trimming of adapters was efficient.

Reads from specimen 915/2804 were mapped against the mitogenome sequence of the white rhinoceros (*Ceratotherium simum*, NC_001808) using BWA v0.7.8 (Li and Durbin, 2009) (aln -l 1024, -n 0.01, -o 2). Reads with a mapping quality Phred score >30 were selected using the SAMtools v1.4 (Li et al., 2009) view command (-q 30), and duplicate reads were discarded using 'FilterUniqueSAMCons.py' (Kircher, 2012). A 50% (majority-rule) consensus sequence was generated from all mapped reads and used as the reference for a subsequent round of mapping. This process was repeated for 26 iterations, until no additional reads could be aligned to the reference. A final 75% consensus sequence was then generated for specimen IPAE915/2804 and checked by eye in Geneious v9.0.4 (Biomatters; http://www.geneious.com), calling nucleotides only for sites covered by ≥3 reads (all other sites coded as N). Reads from specimens IPAE897/123, IPAE2388/1, IPAE2388/5, IPAE1871/200, and IPAE897/200 were mapped against the IPAE915/2804 consensus sequence for three iterations (as described above). Final 75% consensus sequences were then generated as above for specimens IPAE897/123, IPAE2388/1, IPAE2388/5, IPAE1871/200, and IPAE897/200. Details on the mitochondrial genome assemblies can be found in Supplementary Table 2. Consensus sequences for all specimens were very similar (0.2% - 0.3% divergence from 915/2804), though all were unique.

We used MapDamage v.2.0.6 (Jonsson et al., 2013) to ensure that damage patterns in our data were consistent with authentic ancient DNA. With the exception of IPAE2388/1, which had insufficient read depth to return an accurate damage pattern, all libraries displayed damage characteristic of aDNA: high frequency of purines (A and G) in the reference immediately before the beginning of reads, and terminal accumulation of 5' C-to-T and 3' G-to-A misincorporations.

Specimen ID (IPAE)	**915/2804**	**897/123**	**1871/200**	**2388/1**	**897/200**	**2388/5**
ACAD number	15710	15711	15712	15713	15714	15715
GenBank accession	MH937513	MH937514	MH937515	#	MH937516	#
Total number of filtered read pairs	721,051	414,259	445,429	488,971	126,833	559,122
Total number of mapped de-duplicated reads	22,114	1,427	4,746	162	10,290	525
Consensus length (bp)	16,169	16,096	16,128	12,821	16,151	15,963
Consensus coverage (%)	97	92.8	95.9	53.4	96.1	79.3
Mean read length ± standard deviation (bp)	86.5 ± 28.6	80.2 ± 26.2	98.0 ± 39.2	80.3 ± 28.7	90.6 ± 40.0	76.7 ± 27.1
Mean depth of coverage ± standard deviation (X)	113.8 ± 66.3	7.1 ± 4.9	28.8 ± 13.8	0.8 ± 0.9	57.7 ± 26.0	2.5 ± 2.3
No. SNPs compared to 915/2804	-	23	26	3	25	12
Sequence similarity to 915/2804 (%)*	-	99.8	99.8	99.7	99.8	99.8

* Measured as number of unambiguously called nucleotide substitutions compared to 915/2804 divided by total number of unambiguously called nucleotides
# These sequences were too low quality to be uploaded to GenBank, but are instead available on figshare (DOI: 10.25909/5ba34a40ba925)

Supplementary Table 2: *Elasmotherium sibiricum* mitochondrial consensus sequence details

Phylogenetic analyses

We aligned our most complete *Elasmotherium sibiricum* mitogenome sequence (IPAE915/2804) with nine additional published perissodactyl mitogenome sequences (Supplementary Table 3) using the MUSCLE algorithm as implemented in Geneious v9.0.4. We then used PartitionFinder v1.1.1 (Lanfear et al., 2012) to determine the optimal partitioning scheme and substitution models for downstream analysis. We provided PartitionFinder with an input of 32 regions: first and second positions of each individual mitochondrial protein-coding gene; and stem and loop sites of 12S rRNA, 16S rRNA, and concatenated tRNAs. Stem and loop positions of RNA genes were identified using RNAalifold (Bernhart et al., 2008). The best scoring partitioning scheme (according to the BIC) for RAxML (Stamatakis, 2014) comprised five partitions (Supplementary Table 4) while the best scheme for BEAST (Drummond and Rambaut, 2007) analysis comprised six partitions (Supplementary Table 5).

Species name	**Common name**	**Accession**
Ceratotherium simum	White rhinoceros	NC_001808
Coelodonta antiquitatis	Woolly rhinoceros	FJ905813
Dicerorhinus sumatrensis	Sumatran rhinoceros	FJ905816
Diceros bicornis	Black rhinoceros	FJ905814
Elasmotherium sibiricum	“Siberian unicorn”	MH937513
Equus przewalskii	Przewalski’s horse	HQ439484
Hippidion saldiasi	-	KM881671
Rhinoceros sondaicus	Javan rhinoceros	FJ905815
Rhinoceros unicornis	Greater Indian rhinoceros	NC_001779
Tapirus indicus	Asiatic tapir	KJ417808

Supplementary Table 3: Mitochondrial genome sequences included in data matrix for phylogenetic analysis.

Subset	Best model	Subset partitions
1	GTR+G	First codon positions of ATP6, CYTB, ND1, ND2, ND3, ND4L, ND4, and ND5, and second codon positions of ND6
2	GTR+G	Stem positions of 12S & 16S rRNA and tRNAs, and first codon positions of CO1, CO2, and CO3
3	GTR+G	Loop positions of 12S & 16S rRNA and tRNAs, first codon positions of ATP8 and ND6, and second codon positions of ATP8
4	GTR+G	Second codon positions of ATP6, CYTB, ND1, ND2, ND3, ND4L, ND4, and ND5
5	GTR+G	Second codon positions of CO1, CO2, and CO3

Supplementary Table 4: Output from PartitionFinder for analysis in RAxML.

Subset	Best model	Subset partitions
1	GTR+I+G	First codon positions of ATP6, CYTB, ND1, ND3, ND4L, ND4, and ND5, and second codon positions of ND6
2	TrN+G	Loop positions of 12S & 16S rRNA and tRNAs, first codon positions of ATP8, ND2, and ND6, and second codon positions of ATP8
3	TrNef+I	First codon positions of CO1, CO2, and CO3
4	HKY+I+G	Second codon positions of ATP6, CYTB, ND1, ND2, ND3, ND4L, ND4, and ND5
5	HKY+I	Second codon positions of CO1, CO2, and CO3
6	TrN+G	Stem positions of 12S & 16S rRNA and tRNAs

Supplementary Table 5: Output from PartitionFinder for analysis in BEAST.

Our partitioned RAxML v8.2.0 (Stamatakis, 2014) analysis comprised a maximum likelihood search for the best-scoring tree from 1,000 bootstrap replicates (-f a -m MULTIGAMMA -# 1000). We used BEAST v1.8.2 (Drummond and Rambaut, 2007) to simultaneously infer the phylogeny and estimate the timeline for perissodactyl evolution. In our partitioned BEAST analyses, we implemented a Birth-Death tree prior and a single lognormal relaxed clock model (with a rate multiplier parameter for each partition). In order to calibrate our BEAST analysis we constrained the age of two nodes: the divergence between Hippomorpha and Ceratomorpha (uniform distribution between 55.6 mya and 65.5 mya) and

the divergence between Rhinocerotoidea and Tapiroidea (uniform distribution between 52.6 mya and 65.5 mya). The minimum bound on the former constraint was based on *Cymbalophus* from the latest Palaeocene as the earliest unequivocal hippomorph (see Hooker, 2010, 2015). The minimum bound on the latter constraint was based on the earliest unequivocal tapiroid *Heptodon* from the Early Eocene (Holbrook, 1999). The maximum bound for both constraints was based on the absence of perissodactyls from well-sampled North American Palaeocene strata, though it remains possible that the early diversification of perissodactyls occurred elsewhere. We enforced the reciprocal monophyly of Hippomorpha and Ceratomorpha, in accordance with the overwhelming molecular support for these clades (e.g. Meredith et al., 2011). Three independent MCMC chains were run beginning from user-specified random starting trees generated using Mesquite v3.04 (Maddison and Maddison, 2015). Each chain was run for 10^8 generations, and we sampled trees and parameter values every 10^4 generations. The first 10% of samples were discarded as burn-in. Parameter values were monitored and compared between the three independent chains in Tracer v1.6 (http://tree.bio.ed.ac.uk/software/tracer/) to ensure convergence and ESSs >200. We combined sampled trees and parameter values from each BEAST chain before summarising the results.

3. **Stable Isotope analysis at Groningen** (by Margot Kuitems and Hans van der Plicht)

Stable isotope ratios are defined as deviations from the internationally recognized laboratory standard (Equations 1 and 2). For carbon and nitrogen, the material used for this reference standard is Vienna PeeDee Belemnite (VPDB) and ambient inhalable reservoir (AIR) respectively (Mook, 2006). The analytical error is 0.3 ‰ for $\delta^{13}C$ and 0.2 ‰ for $\delta^{15}N$.

Equation 1

$$^{13}\delta = \frac{(^{13}C/^{12}C)_{sample}}{(^{13}C/^{12}C)_{reference}} - 1(\times 1000‰)$$

Equation 2

$$^{15}\delta = \frac{(^{15}N/^{14}N)_{sample}}{(^{15}N/^{14}N)_{reference}} - 1(\times 1000‰)$$

Stable isotope data are reported in Supplementary Table 6, and plotted against latitude and calibrated median radiocarbon age of samples in Supplementary Fig. 1 (see main text for discussion).

Species	Locality	specimen	%C	%N	C:N	$\delta^{13}C$ (‰)	$\delta^{15}N$ (‰)	Reference
Elasmotherium sibericum	Smelovskya	IPAE 420/111	*35.9*	*15.2*	*2.8*	*−15.8*	*11.0*	*this work; Groningen*
Elasmotherium sibericum	Tobolsk	IPAE 915/2805	42.2	16.0	3.2	−18.8	12.8	this work; Oxford
Elasmotherium sibericum	Bashkiriya	IPAE 2388/2	45.0	16.2	3.2	−16.4	9.6	this work; Groningen
Elasmotherium sibericum	Samara district	ZIN 31791	41.8	15.6	3.1	−17.2	9.6	this work; Groningen
Elasmotherium sibericum	Bashkiriya	IPAE 2388/1	47.8	17.2	3.2	−17.8	6.5	this work; Groningen
Elasmotherium sibericum	Samara district	IPAE 17-5703/7	42.9	15.5	3.2	−17.3	8.8	this work; Groningen
Elasmotherium sibericum	Samara district	IPAE 5-147	42.0	15.1	3.2	−17.7	10.2	this work; Groningen
Elasmotherium sibericum	Samara district	IPAE 12-001	41.3	15.0	3.2	−18.7	10.0	this work; Groningen
Elasmotherium sibericum	Samara district	IPAE 10-5566	42.2	15.4	3.2	−21.5	8.4	this work; Groningen
Elasmotherium sibericum	Borovlyanka	IPAE 897/200	43.4	17.1	3.0	−18.8	9.4	this work; Groningen
Elasmotherium sibericum	Sarepta	NHM M12429	46.4	17.0	3.2	−16.3	7.8	this work; Groningen

Elasmotherium sibericum	unknown	ZIN 36331	45.2	16.7	3.2	−16.9	10.3	this work; Groningen
Elasmotherium sibericum	Luchka	ZIN (26021) 3963	42.3	15.6	3.2	−18.2	10.1	this work; Groningen
Elasmotherium sibericum	Incineration factory	ZIN 3986	43.3	15.9	3.2	−17.8	7.2	this work; Groningen
Elasmotherium sibericum	Bashkiriya	IPAE 2388/3	45.4	17.5	3.0	−18.2	10.4	this work; Groningen
Elasmotherium sibericum	Saratov	NHM M7099	45.0	16.5	3.2	−17.3	11.6	this work; Groningen
Elasmotherium sibericum	Voronovka	IPAE 1871/200	45.4	16.6	3.2	−18.7	8.6	this work; Groningen
Elasmotherium sibericum	Borovlyanka	IPAE 897/172	43.5	16.3	3.1	−18.6	9.6	this work; Groningen
Elasmotherium sibericum	Luchka	ZIN 10794	44.3	16.4	3.2	−18.3	9.5	this work; Groningen
Elasmotherium sibericum	Bashkiriya	IPAE 2388/5	44.4	16.9	3.1	−19.2	7.2	this work; Groningen
Elasmotherium sibericum	Irbit	C/M 12836	48.4	17.6	3.2	−17.4	10.1	this work; Groningen
Elasmotherium sibericum	Hydroelectric Power Station	ZIN 36330	32.4	11.9	3.2	−16.6	10.4	this work; Groningen
Elasmotherium sibericum	Borovlyanka	IPAE 897/123	35.2			−20.9		this work; Groningen
Stephanorhinus kirchbergensis	Schöningen, Germany	FID 13689				-22.1	6.4	Kuitems *et al*. 2015
Stephanorhinus kirchbergensis	Schöningen, Germany	Fnr 738/10				-22.4	5.7	Kuitems *et al*. 2015
Stephanorhinus cf *S. kirchbergensis*	Schöningen, Germany	Fnr 715/**2**				-22.7	6.5	Kuitems *et al*. 2015
Stephanorhinus cf *S. kirchbergensis*	Schöningen, Germany	Fnr 298/4				-22.9	3.7	Kuitems *et al*. 2015
Stephanorhinus sp.	Schöningen, Germany	FID 16817				-23.6	3.4	Kuitems *et al*. 2015
Stephanorhinus sp.	Schöningen, Germany	FID 14834				-20.4	3.1	Kuitems *et al*. 2015
Stephanorhinus sp.	Schöningen, Germany	Fnr 679/0-1				-20.4	3.8	Kuitems *et al*. 2015
Coelodonta antiqitatis	Grotto Rasik, Urals	IPAE-888/114				-19.7	4.2	Stuart and Lister 2012
Coelodonta antiqitatis	Grotto Kumishsky, Urals	IPAE-910/397				-19.6	5.4	Stuart and Lister 2012
Coelodonta antiqitatis	Gr. Cheremuhovo 1-4, Urals	IPAE-993/1870				-19.5	5.1	Stuart and Lister 2012
Coelodonta antiquitatis	Nizhnie Gari, Urals	IPAE-781/112				-19.5	4.9	Stuart and Lister 2012
Coelodonta antiquitatis	Isimo River, Sokolovka Region	ORAU lab # OxA-12072				-19.3	8.1	Stuart and Lister 2012
Coelodonta antiquitatis	Duruitoarea Veche	ORAU lab # OxA-11690				-19.4	7.2	Stuart and Lister 2012
Coelodonta antiquitatis	Urovsk, Urals	IPAE-577/532				-19.2	5.0	Stuart and Lister 2012
Cœlodonta antiquitatis	Cheremiskoe	IPAE-1106/1				-18.6	6.1	Stuart and Lister 2012
Saiga tatarica	Chelyabinsk Region	ZIN 21049				-17.6	9.0	Jürgensen *et al*. 2017
Saiga tatarica	Volga River near Luchka	ZIN 1084				-17.4	8.2	Jürgensen *et al*. 2017
Saiga tatarica	Mostovskiy District, Barakaevs	ZIN Barakov				-18.6	7.6	Jürgensen *et al*. 2017
Saiga tatarica	Buran-Kaya III, Crimea	9Z-1054				-15.5	10.0	Jürgensen *et al*. 2017
Saiga tatarica	Buran-Kaya, Crimea	BK3-07-2				-15.6	9.5	Jürgensen *et al*. 2017
Saiga tatarica	Buran-Kaya, Crimea	BK3os-10-02				-17.6	7.0	Jürgensen *et al*. 2017
Saiga tatarica	Buran-Kaya, Crimea	BK3os-10-03				-16.5	10.9	Jürgensen *et al*. 2017

Supplementary Table 6: Stable isotope measurements ($\delta^{13}C$ and $\delta^{15}N$ values, %C and %N, and the atomic C:N ratio that indicates the integrity of the collagen). The C:N ratio of sample IPAE 420/111 (in italics) is just outside the range of reliable values indicative for good bone collagen.

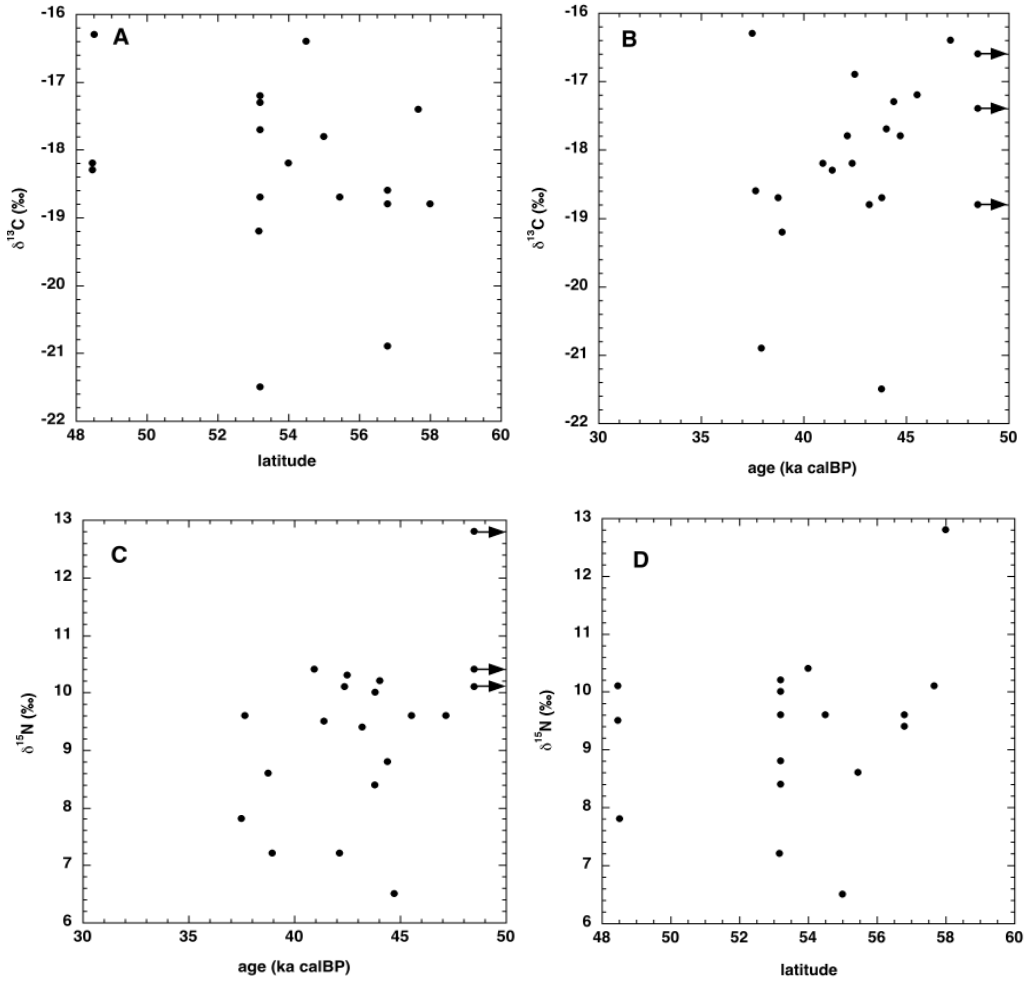

Supplementary Figure 1: Stable isotope values of *E*. *sibiricum* versus latitude and radiocarbon age: (A) δ^{13}C versus latitude of samples; (B) δ^{13}C versus calibrated radiocarbon date of samples; (C) δ^{15}N versus calibrated radiocarbon date of samples; (D) δ^{15}N versus latitude of samples. Data from Supplementary Tables 1 & 6.

4. Chronometric data obtained at the ORAU (by Thibaut Devièse and Tom Higham)

Sample no.	P-code	% Yield	%C	C:N	δ^{13}C‰	δ^{15}N‰	CRA (BP)	±	OxA number
C/M 12836	AF	/	45.3	3.3	-17.4	10.2	29500	330	OxA-V-2754-19
	AF	/	43.4	3.3	-17.2	10.2	29290	320	OxA-V-2754-18
	HYP	/	42.7	4.8	-32.6	-5.8	>51100		OxA-X-2750-15
	HYP	/	46.4	4.8	-29.6	-2.1	>49000		OxA-X-2750-14
NHM M7099	AF	2.1	42.8	3.4	-16.9	11.7	31650	400	OxA-29557
	HYP	/	40.5	5.0	-22.4	15.3	>45700		OxA-X-2762-57
ZIN 36330	AF	7.4	43.1	3.2	-19.1	8.1	38300	900	OxA-36749
	HYP	/	46.8	4.8	-26.6	-11.4	50300	2700	OxA-X-2750-38
ZIN 10794	AF	/	42.5	3.2	-18.4	9.7	33040	340	OxA-V-2754-17
	HYP	/	44.1	4.9	-28.9	0.2	36850	650	OxA-X-2750-13
IPAE 2388/5	AF*	4.7	43.4	3.4	-18.7	7.5	31850	400	OxA-31828
	HYP	/	36.2	5.1	-25.7	10.3	34400	1000	OxA-X-2756-57
IPAE 1871/200	AF*	6.1	44.0	3.3	-17.8	9.8	34500	600	OxA-31896
	HYP	/	30.4	5.0	-15.8	15.1	34250	700	OxA-X-2677-55
IPAE 897/172	AF*	7.1	45.4	3.3	-18.2	8.8	34200	550	OxA-31827
	HYP	/	31.0	5.2	-24.7	8.8	33300	1100	OxA-X-2756-56
IPAE 897/123	AF*	3.1	42.8	3.4	-18.8	8.9	33450	500	OxA-31826
	HYP	/	32.8	5.0	-22.7	11.7	33650	650	OxA-X-2677-54
NHM M12429	AF	7.4	45.1	3.3	-16.1	8.3	32250	450	OxA-28220
	HYP	/	38.0	5.0	-22.6	11.3	33250	500	OxA-X-2677-52
IPAE 915/2804	AF	10.7	42.2	3.2	-18.8	12.8	>49200		OxA-34900

Supplementary Table 7: Chronometric data for 10 of the Elasmotherium samples dated at the ORAU. PCode refers to pretreatment code; '**AF**' is ultrafiltered collagen; '**HYP**' denotes the extraction of hydroxyproline from hydrolysed bone collagen. Samples that had been preserved with glues, or samples for which we did not have complete knowledge of their post-excavation history, were also washed with solvents (acetone, methanol and chloroform) prior to AF treatment (coded '**AF***'). %Yield is the percent yield of extracted collagen as a function of the starting weight of the bone analysed. When further purification (AF or HYP) was performed on previously extracted collagen, the yields are not reported. All samples were prepared and dated at the ORAU with the exception of C/M12836 and ZIN 10794. Collagen from these 2 samples was extracted at the University of Groningen and dated in Oxford after adding the ultrafiltration step (coded OxA-V). %C is the carbon present in the combusted sample (gelatin or hydroxyproline). C/N is the atomic ratio of carbon to nitrogen and is acceptable if it ranges between 2.9—3.5 in the case of collagen or ~5.0 in the case of hydroxyproline. Stable isotope ratios are expressed in per mil (‰) relative to vPDB with a mass spectrometric precision of ±0.2‰ (Coplen Tyler 1994). CRA is conventional radiocarbon age, expressed in years BP (Stuiver and Polach 1977). For all HYP dates, the background carbon derived from the HPLC separation has been subtracted using a correction calculation described in (Devièse et al. 2018).

Museums & Specimen references	Groningen dates	Oxford AF/AF* dates	Oxford HYP dates	Chi squared results	
				GrA versus AF/AF*	AF/AF* versus HYP
C/M 12836	29740 ± 145 (GrA-53428)	29500 ± 330 (OxA-V-2754-19)	> 51100 (OxA-X-2750-15)	Pass (T=0.44)	Fail
		29290 ± 320 (OxA-V-2754-18)	> 49000 (OxA-X-2750-14)	Pass (T=1.64)	Fail
NHM M7099	33630 ± 215 (GrA-62353)	31650 ± 400 (OxA-29557)	> 45700 (OxA-X-2762-57)	Fail (T=19.01)	Fail
ZIN 36330	28650 ± 160 (GrA-62204)	38300 ± 900 (OxA-36749)	50300 ± 2700 (OxA-X-2750-38)	Fail (T=111.44)	Fail (T=17.78)
ZIN 10794	32410 ± 200 (GrA-62198)	33040 ± 340 (OxA-V-2754-17)	36850 ± 650 (OxA-X-2750-13)	Pass (T=2.55)	Fail (T=26.98)
IPAE 2388/5	31040 ± 175 (GrA-55453)	31850 ± 400 (OxA-31828)	34400 ± 1000 (OxA-X-2756-57)	Pass (T=3.44)	Fail (T=5.61)
IPAE 1871/200	33620 ± 210 (GrA-53426)	34500 ± 600 (OxA-31896)	34250 ± 700 (OxA X-2677-55)	Pass (T=1.92)	Pass (T=0.07)
IPAE 897/172	33380 ± 205 (GrA-53424)	34200 ± 550 (OxA-31827)	33300 ± 1100 (OxA-X-2756-56)	Pass (T=1.95)	Pass (T=0.54)
IPAE 897/123	22180 ± 95 (GrA-52426)	33450 ± 500 (OxA-31826)	33650 ± 650 (OxA X-2677-54)	Fail (T=490.35)	Pass (T=0.06)
NHM M12429	39020 ± 215 (GrA-62354)	32250 ± 450 (OxA-28220)	33250 ± 500 (OxA X-2677-52)	Fail (T=184.27)	Pass (T=2.21)

Supplementary Table 8: χ^2 test results on radiocarbon dates obtained in Groningen and Oxford. The statistical analysis was done using the OxCal 4.3 platform (Ramsey 2018), following Ward and Wilson (1978). The error weighted mean and the T values were calculated for each pair of samples. If T is < 3.84, the error-weighted mean is not significant at the 0.05 level and the two dates are therefore not statistically distinguishable.

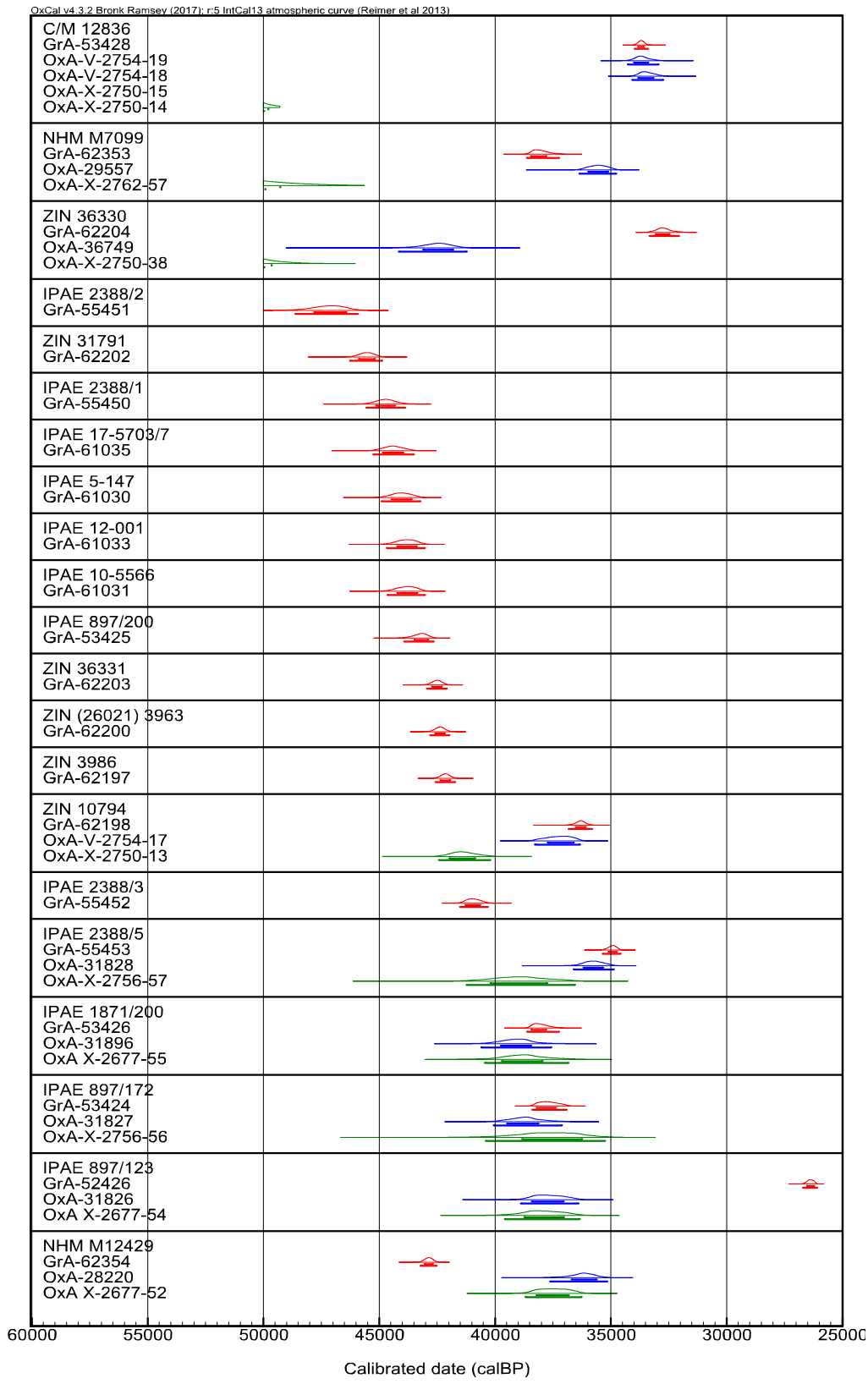

Supplementary Figure 2: Oxcal output showing the full probability distributions for all the calibrated dates of the 21 Elasmotherium samples. The calibration curve of Reimer et al. (2013) was used to calibrate the results. The dates represented in red were obtained in the Groningen radiocarbon lab while the dates in blue and green were obtained at the ORAU in Oxford. Dates in blue were obtained on ultrafiltered collagen and dates in green were obtained on hydroxyproline (see methods section).

	Unmodelled (BP)				Modelled (BP)			
	68.20%		95.40%		68.20%		95.40%	
	From	to	From	to	From	to	From	to
Start boundary					50160	47260	51320	46390
OxA-X-2750-38	...	49640	...	49950	49980	47150	50010	45820
GrA-55451	47800	46420	48630	45920	47670	46310	48490	45810
GrA-62202	45880	45180	46260	44860	45880	45160	46290	44840
GrA-55450	45140	44310	45560	43870	45170	44290	45580	43840
GrA-61035	44860	43960	45260	43500	44880	43950	45280	43470
GrA-61030	44470	43590	44910	43220	44510	43560	44940	43210
GrA-61033	44230	43370	44670	43040	44280	43350	44710	43020
GrA-61031	44210	43350	44660	43020	44250	43340	44700	42990
GrA-53425	43480	42870	43920	42640	43500	42860	43970	42630
GrA-62203	42720	42280	42940	42080	42720	42280	42950	42080
GrA-62200	42580	42160	42800	41970	42600	42170	42820	41950
GrA-62197	42360	41930	42570	41720	42360	41930	42600	41710
OxA-X-2750-13	41980	40860	42430	40200	41990	40840	42430	40180
GrA-55452	41280	40630	41530	40300	41280	40600	41590	40240
OxA-X-2756-57	40200	37740	41230	36540	40150	37860	41310	36950
OxA-X-2677-55	39710	37950	40440	36820	39760	38020	40490	37050
OxA-X-2656-56	38830	36230	40400	35240	39440	37040	40740	36270
OxA-X-2677-54	38730	37010	39570	36340	38970	37370	39720	36680
OxA-X-2677-52	38220	36810	38690	36260	38500	37230	38900	36490
End boundary (Extinction)					**37960**	**36170**	**38480**	**34950**

Supplementary Table 9: Estimation of the extinction date of *Elasmotherium sibiricum*. This is a simple 'Phase' model in OxCal 4.3 in which all determinations are assumed to have no relative order. "Start" and "End" correspond to the boundaries calculated by the model. All dates have been rounded to the closest 10.

5. Code used to calibrate the 14C ages in OxCal

```
Plot()
 {
  Outlier_Model("General",T(5),U(0,4),"t");
  Sequence()
  {
   Boundary("Start of 14C series");
   Phase("1")
   {
    R_Date("OxA-X-2750-38", 50300, 2700)
    {
     Outlier("General", 0.05);
    };
    R_Date("GrA-55451", 43900, 575)
    {
     Outlier("General", 0.05);
    };
    R_Date("GrA-62202", 42230, 370)
    {
     Outlier("General", 0.05);
    };
    R_Date("GrA-55450", 41220, 445)
    {
     Outlier("General", 0.05);
    };
    R_Date("GrA-61035", 40860, 455)
    {
     Outlier("General", 0.05);
    };
    R_Date("GrA-61030", 40470, 445)
    {
     Outlier("General", 0.05);
    };
    R_Date("GrA-61033", 40200, 445)
    {
     Outlier("General", 0.05);
    };
    R_Date("GrA-61031", 40180, 445)
    {
     Outlier("General", 0.05);
    };
    R_Date("GrA-53425", 39480, 355)
    {
     Outlier("General", 0.05);
    };
    R_Date("GrA-62203", 38440, 295)
    {
     Outlier("General", 0.05);
    };
    R_Date("GrA-62200", 38230, 285)
    {
```

```
   Outlier("General", 0.05);
  };
  R_Date("GrA-62197", 37850, 285)
  {
   Outlier("General", 0.05);
  };
  R_Date("OxA-X-2750-13", 36850, 650)
  {
   Outlier("General", 0.05);
  };
  R_Date("GrA-55452", 36290, 275)
  {
   Outlier("General", 0.05);
  };
  R_Date("OxA-X-2756-57", 34400, 1000)
  {
   Outlier("General", 0.05);
  };
  R_Date("OxA-X-2677-55", 34250, 700)
  {
   Outlier("General", 0.05);
  };
  R_Date("OxA-X-2656-56", 33300, 1100)
  {
   Outlier("General", 0.05);
  };
  R_Date("OxA-X-2677-54", 33650, 650)
  {
   Outlier("General", 0.05);
  };
  R_Date("OxA-X-2677-52", 33250, 500)
  {
   Outlier("General", 0.05);
  };
 };
 Boundary("Extinction");
};
};
```

Supplementary References (additional to those cited in main text)

Aerts A.T., J. van der Plicht, H.A.J. Meijer, 2001. Automatic AMS sample combustion and CO_2 collection. Radiocarbon 43, 293-298.

Borodin, A., Markova, E., Zinovyev, E., Strukova, T., Fominykh, M., Zykov, S., 2013. Quaternary rodent and insect faunas of the Urals and Western Siberia: connection between Europe and Asia. Quaternary International 284, 132-150.

Bernhart, S., Hofacker, I., Will, S., Gruber, A., Stadler, P., 2008. RNAalifold: improved consensus structure prediction for RNA alignments. BMC Bioinformatics 9, 474.

Coplen Tyler B (1994) Reporting of stable hydrogen, carbon, and oxygen isotopic abundances (Technical Report). in *Pure and Applied Chemistry*, pp 273-276.

Dabney, J., Knapp, M., Glocke, I., Gansauge, M. T., Weihmann, A., Nickel, B., ... & Meyer, M. 2013. Complete mitochondrial genome sequence of a Middle Pleistocene cave bear reconstructed from ultrashort DNA fragments. Proceedings of the National Academy of Sciences, 201314445.

Danukalova, G.A., Yakovlev, A.G., Alimbekova, L.I., Eremeev, A.A., Morozova, E.M., Kosintcev, P., Agadjanian, A., 2009. Quaternary fauna and flora of the Southern Urals region (Bashkortostan Republic). Quaternary International 201, (1/2): 13 – 24.

Grichuk, V.P., 2002. Vegetation of the Late Pleistocene. In: Dynamics of terrestrial landscape components and inner marine basins of Northern Eurasia during the last 130 000 years. (Ed. A.A.Velichko). Moscow: GEOS Publishers, 64-88. (in Russian).

Holbrook, L.T., 1999. The Phylogeny and Classification of Tapiromorph Perissodactyls (Mammalia). Cladistics 15, 331-350.

Hooker, J.J., 2010. The mammal fauna of the Early Eocene Blackheath Formation at Abbey Wood, London. Monogr Palaeontogr Soc 634, 1-162.

Hooker, J.J., 2015. A two-phase mammalian dispersal event across the Paleocene-Eocene boundary. Newsl Stratigr 48, 201-220.

Ivakina, N.V., Strukova, T.V., Borodin, A.V., Stefanovsky, V.V., 1999. Some of the material on the formation of modern ecosystems of the Middle and South Urals. Paleontological Journal 31 (3): 272-276. (in Russian).

Jonsson, H., Ginolhac, A., Schubert, M., Johnson, P.L., Orlando, L., 2013. mapDamage2.0: fast approximate Bayesian estimates of ancient DNA damage parameters. Bioinformatics 29, 1682-1684.

Khromov, A.A., 1999. About the remains of Elasmotherium from the funds of the Saratov regional Museum. Paleontological Journal 33 (1): 116-122. (in Russian).

Khromov, A.A., Arkhangelskii, M.S., Ivanov, A.V., 2000. The location of Quaternary large mammals in the Saratov Volga region. Saratov: Scientific book, 156 p. (in Russian).

Khromov, A.A., Arkhangelskii, M.S., Ivanov, A.V., 2001. Large Quaternary mammals of Middle and Lower Volga region. Dubna: Publishing house of University "Dubna", 254 p. (in Russian).

Kircher, M., 2012. Analysis of High-Throughput Ancient DNA Sequencing Data. Ancient DNA: Methods and Protocols, pp. 197-228.

Kosintsev, P.A., Bachura, O.P., 2013. Late Pleistocene and Holocene mammal fauna of the Southern Urals. Quaternary International 284, 161 – 170.

Kosintsev, P.A., Vasiliev, S.K., 2009. The Large mammal fauna in the Neopleistocene of Western Siberia. Bulletin of Comission for study of the Quarternary 69, 94-105. (in Russian).

Kosintsev, P.A., Bobkovskaya, N.E., 2003. Neopleistocene megamammals from the latitudinal part of the Irtysh-river reaches. In: Quaternary paleozoology in the Urals (Ed. Smirnov N.). Ekaterinburg: Publishing house of the Ural University, 226-232. (in Russian).

Lanfear, R., Calcott, B., Ho, S.Y.W., Guindon, S., 2012. PartitionFinder: combined selection of partitioning schemes and substitution. Mol Biol Evol 29, 1537-1719.

Lindgreen, S., 2012. AdapterRemoval: easy cleaning of next-generation sequencing reads. BMC Research Notes 5, 337.

Longin, R. 1971. New method of collagen extraction for Radiocarbon dating. Nature 230, 241-242.

Maddison, W.P., Maddison, D.R., 2015. Mesquite: a modular system for evolutionary analysis. Version 3.04 http://mesquiteproject.org.

Markova, A.K., Simakova, A.N., Puzachenko, A.Y., Kitaev, L.M., 2002. Environments of the Russian Plain during the Middle Valdai Briansk Interstadial (33,000-24,000 yr B.P.) indicated by fossil mammals and plants. *Quaternary Research* 57(3): 391-400.

Markova, A.K., Puzachenko, A.Yu., Kolfschoten, T. van, 2008. Species composition and geographical position of the mammal assemblages in the North Eurasia during the end of middle Valdai (=middle Zyrianian- middle Vistulian) mega-interstadial. In: Faunae and Florae of Northern Eurasia in the Late Cenozoic (Ed. Kosintsev P.), 7-24. (in Russian).

Mitchell, K.J., Bray, S.C., Bover, P., Soibelzon, L., Schubert, B.W., Prevosti, F., Prieto, A., Martin, F., Austin, J.J., Cooper, A., 2016a. Ancient mitochondrial DNA reveals convergent evolution of giant short-faced bears (Tremarctinae) in North and South America. Biol Lett 12.

Mitchell, K.J., Scanferla, A., Soibelzon, E., Bonini, R., Ochoa, J., Cooper, A., 2016b. Ancient DNA from the extinct South American giant glyptodont Doedicurus sp. (Xenarthra: Glyptodontidae) reveals that glyptodonts evolved from Eocene armadillos. Mol Ecol 25, 3499-3508.

Mook W.G., 2006. Introduction to Isotope Hydrology. Taylor and Francis, London. ISBN 0415381975.

Mook W.G., J. van der Plicht, 1999. Reporting ^{14}C activities and concentrations. Radiocarbon 41, 227-239.

Ramsey C.B., 2018. OxCal Analysis. *OxCal 43 Manual*. Available at: http://c14.arch.ox.ac.uk/oxcalhelp/hlp_analysis.html [Accessed May 18, 2018].

Reimer, P.J., E. Bard, A. Bayliss, J.W. Beck, P.G. Blackwell, C. Bronk Ramsey, C.E. Buck, R.L. Edwards, M. Friedrich, P.M. Grootes, T.P. Guilderson, H. Haflidason, I. Hajdas, C. Hatté, T.J. Heaton, D.L. Hoffmann, A.G. Hogg, K.A. Hughen, K.F. Kaiser, Bernd Kromer, S.W. Manning, M. Niu, R.W. Reimer, D.A. Richards, E.

M. Scott, J.R. Southon, R.A. Staff, C.S.M. Turney, J. van der Plicht, 2013. IntCal13 and Marine13 Radiocarbon age calibration curves 0-50,000 years cal BP. Radiocarbon 55, 1869-1887.

Shilova, G.N., Demidova, A.N., Tevelev, A.V., 2008. Quaternary evolution of plant communities of the southern Urals. In: Palynology: stratigraphy and geoecology (Eds. Prischepa O.M., Subetto D.A., Dzyuba O.F.), v. 2. Sankt-Petersburg 264-270. (in Russian).

Shirokov, V.N., Volkov, R.B., Kosintsev, P.A., Lapteva, E.G., 2011. Paleolithic site Bogdanovka (South Urals). Russian archeology 1, 125-139. (in Russian).

Sinitsyn, A.A., N.D. Praslov (eds.), 1997. Radiocarbon chronology of the Upper Paleolithic of Eastern Europe and Northern Asia: Problems and perspectives. St.-Petersburg: Academprint Publishing House, 21-66. (in Russian).

Stefanovsky, V.V., Zinovyev, E.V., Trofimova, S.S., Strukova, T., 2002. Nikitino – parastratotype section of Rejevskoi alluvial complex of the Middle Urals. Ural geological journal 25 (1): 7-19. (in Russian).

Stefanovsky, V.V., Borodin, A.V., Strukova, T.V., 2003. Correlation of the Upper Neopleistocene alluvial and lacustrine sections, the southern trans-Urals region. Stratigraphy and Geological Correlation 11 (4): 391-403.

Stefanovsky, V.V., Zinovyev, E.V., Trofimova, S.S., 2007. The alluvial complexes in lower reaches of the river Tavda (Northern Urals). Ural geological journal 56 (2): 5-25. (in Russian).

Stuiver M & Polach HA (1977) Discussion: Reporting of C-14 data. *Radiocarbon* 19(3):355-363.

van der Plicht, J., S. Wijma, A.T. Aerts, M.H. Pertuisot, H.A.J. Meijer, 2000. The Groningen AMS facility : status report. Nuclear Instruments and Methods B172, 58-65.

Ward, G.K., Wilson, S.R. 1978. Procedures for comparing and combining radiocarbon age determinations: a critique. *Archaeometry* 20(1):19–31.

Zinovyev, E.V., 2003. Sites of Quaternary insects in the Urals and Trans-Urals. In: Quaternary paleozoology in the Urals (Ed. Smirnov N.). Ekaterinburg: Publishing house of the Ural University, 86 – 97. (in Russian).

Zinovyev, E.V., 2011. Sub-fossil beetle assemblages associated with the “mammoth fauna” in the Late Pleistocene localities of the Ural Mountains and West Siberia. ZooKeys, 100, 149–169.

Supplementary Table (.xls file)

Supplementary Table 1: Specimen numbers, localities, and summary of radiocarbon results. Raw radiocarbon dates are quoted ± 1-sigma; calibrated dates as 2-sigma range rounded to the nearest 10.